Structural Events in the Photocycle of Green Fluorescent Protein

Jasper J. van Thor,*,† Giulia Zanetti,† Kate L. Ronayne,‡ and Michael Towrie‡

Laboratory of Molecular Biophysics, University of Oxford, Rex Richards Building, South Parks Road, Oxford OX1 3QU, United Kingdom, and Central Laser Facility, CCLRC Rutherford Appleton Laboratory, Chilton, Didcot, Oxfordshire, OX11 0QX, United Kingdom

Received: March 14, 2005; In Final Form: June 21, 2005

Picosecond time-resolved mid-infrared absorption changes of the wild type green fluorescent protein from *Aequorea victoria* are reported on structural events during the photocycle. Concomitant with rapid H/D transfer following excitation of the neutral *A* state at 400 nm, a transient signal at 1721/1711 cm^{-1} (H/D) developed belonging to protonated glutamate 222, which was definitively assigned using the E222D mutant from the altered proton-transfer kinetics to aspartate in addition to the altered band position and intensity in the spectra. A transient at 1697 cm^{-1}, assigned to a structural perturbation of glutamine 69, had a H/D kinetic isotope effect of >32, showing the conformational dynamics to be sensitive to the active site H/D vibrations. The kinetic data up to 2 ns after excitation in the 1250−1800 cm^{-1} region in D_2O provided 10 and 75 ps time constants for the excited-state deuteron transfer and the associated $A_1^* - A_1$ and $A_2^* - A_2$ difference spectra and showed the radiative intermediate *I** state vibrations and the transient accumulation of the long-lived ground-state intermediate I_2. Assignments of chromophore modes for the A_1, A_2, and I_2 ground states are proposed on the basis of published model compound studies[1,2] (Esposito, A. P.; Schellenberg, P.; Parson, W. W.; Reid, P. J. *J. Mol. Struct.* **2001**, *569*, 25 and He, X.; Bell, A. F.; Tonge, P. J. *J. Phys. Chem. B* **2002**, *106*, 6056). Tentative assignments for the singlet-state intermediates A_1^*, A_2^*, and *I** are discussed. An unexpected and unassigned band that may be a C═C chromophore vibration was observed in the ground state (1665 cm^{-1}) as well as in all photocycle intermediates. Optical dumping of the transient *I** population was achieved using an additional 532 nm pulse and the directly obtained $I_2 - I^*$ difference spectrum was highly similar to the $I_2 - I^*$ photocycle spectrum. The pump−dump−probe spectrum differed from the pump−probe photocycle difference spectrum with respect to the intensity of the phenol 1 mode at 1578 cm^{-1}, suggesting stronger delocalization of the negative charge onto the phenolic ring of the anionic chromophore in the dumped I_2 state. Indication for structural heterogeneity of the chromophore, Glu 222, and the chromophore environment was found in the two parallel proton-transfer reactions and their distinct associated ground- and intermediate-state vibrations. Vibrational spectral markers at 1695 cm^{-1} assigned to Gln 69, at 1631 cm^{-1} belonging to a C═C mode, and at 1354 cm^{-1} belonging to a phenolate vibration further indicated the I_2 and *I** states to be unrelaxed.

Introduction

The fluorescence and structural properties of the wild type green fluorescent protein (GFP) from *Aequorea victoria* have been investigated extensively.[3−5] The *p*-hydroxybenzylidene-imidazolinone chromophore is formed via the internal cyclization in the backbone of the Ser-Tyr-Gly sequence.[6] At pH 8, GFP exists mostly in the neutral ground-state *A*, with the phenolic oxygen protonated,[3,7] which absorbs maximally at 398 nm. The absorption spectrum of wt-GFP shows an additional minor contribution at 478 nm corresponding to the anionic *B* ground state.[8] Optical excitation of the *A* state at 400 nm produces the *A** state, which rapidly deprotonates with 2 and 11 ps (12 and 69 ps in D_2O) time constants to form the radiative photocycle intermediate *I**, which has a lifetime of 3 ns.[4,9−11] The excited-state deprotonation follows the Förster cycle, which describes the reduction of the proton affinity for the optically excited state.[12] The H/D kinetic isotope effect (KIE) for this step was shown to be approximately 6.[4,9] It was proposed that the corresponding deprotonated ground-state *I* would be a photocycle intermediate but could not be observed.[4,11,13] Hole-burning products assumed to be *I* ground states were observed in low-temperature spectra.[13,15] Recently, two new photocycle intermediate states were described, designated I_1 (500 nm) and I_2 (497 nm), which have lifetimes of 3 ps (7 ps) and 400 ps (5 ns) in H_2O (D_2O).[9] The I_1 and I_2 intermediates do not accumulate significantly in H_2O. However, in D_2O, the I_2 state transiently accumulates to an observable level due to the H/D KIE = 12 for the $I_2 \rightarrow A$ ground-state recovery. Population inversion of the transient *I** state using the pump−dump−probe technique created the I_1 ground-state intermediate, and its subsequent decay to the long-lived I_2 intermediate could be observed.[9] The blue-shift and moderate KIE for the $I_1 \rightarrow I_2$ transition has been interpreted to reflect a structural relaxation involving both chromophore and protein relaxation in addition to solvent reorganization.[9,14] Several proposals have been put forward for the excited-state proton acceptor, including His 148,[5,16] Glu 222,[14,17−19] potentially bulk solvent,[20] and the

* To whom correspondence should be addressed. E-mail: Jasper@biop.ox.ac.uk; phone: +44 (0)1865 285352; fax: +44 (0)1865 275182.
† University of Oxford.
‡ CCLRC Rutherford Appleton Laboratory.

10.1021/jp051315+ CCC: $30.25
Published on Web 08/04/2005

involvement of a proton-transfer pathway including Glu 222, Asp 82, and Glu 5.[21]

Recent experimental evidence from picosecond time-resolved mid-infrared spectroscopy strongly suggested Glu 222 as the excited-state proton acceptor in the fluorescence photocycle.[14,19] In addition, a transient at 1697 cm^{-1} was assigned to structural perturbation of Gln 69, which was detected on the early time scale together with the 1711 cm^{-1} transient.[14] Temperature-dependent structural relaxation of the chromophore environment upon chromophore ionization was observed after phototransformation at cryogenic temperatures. Stable phototransformation at 100 K, which leads to decarboxylation of Glu 222, produces an early lumi photoproduct GFP_L, which absorbs maximally at 497 nm. GFP_L shows characteristic IR absorption changes relative to the neutral *A* state, GFP_A, as well as strong structural changes of protein and solvent in the chromophore environment, as determined by X-ray crystallography.[14] Structural annealing of GFP_L at 200 K produces a meta-stable intermediate GFP_M, which absorbs at 482 nm and shows characteristic IR absorption changes relative to GFP_L. In particular, a phenol mode at 1362 cm^{-1} in GFP_L shifts to 1341 cm^{-1} in GFP_M, signaling relaxation of the chromophore environment. Both GFP_L and GFP_M intermediates show a protein vibration at 1697 cm^{-1}, belonging to the electrostatically driven structural perturbation of Gln 69. The assignment of the 1697 cm^{-1} band to Gln 69 was made from the X-ray structures of GFP_L and GFP_M and was confirmed by its absence in the FTIR spectrum of the phototransformed Q69L/T203H mutant at 100 K. Picosecond time-resolved transient infrared absorption spectroscopy showed the appearance of the 1697 cm^{-1} band belonging to Gln 69 in the fluorescence photocycle intermediate *I**, demonstrating a similar structural response to chromophore ionization in both phototransformation and fluorescence pathways. The electrostatic response of the protein and solvent to optical excitation and charge transfer to the chromophore was proposed to be important for inhibiting nonradiative decay, explaining the very high quantum yield of fluorescence (0.8) in view of the formation of a buried charge.[14]

Phototransformation at 300 K of the *A* state using either blue- or UV-light leads to the irreversible formation of an anionic species GFP_R.[7,14,22] The vibrational response to the phototransformation, which results in deprotonation of the chromophore, was addressed by difference FTIR spectroscopy.[7,14] The difference FTIR spectra between neutral and anionic ground states show strong bands in the mid-infrared region between 1000 cm^{-1} and 1750 cm^{-1} and are dominated by chromophore modes, including a number of strong bands at 1580, 1538, 1497, 1342, 1316, and 1147 cm^{-1} in H_2O belonging to the phenolate product state.[7,14] Calculation of the IR intensities in the mid-infrared region of the anionic form of a chromophore model compound using restricted Hartree−Fock geometry showed several modes to be more intense than the corresponding modes of the neutral chromophore.[23] On the basis of similar calculations, assignments were proposed for the neutral ground state of the GFP chromophore model compound 4-hydroxybenzylidene-1,2-dimethylimidazolinone (HBDI) in the high-frequency region 1700−1430 cm^{-1} for infrared as well as Raman active modes.[1] Infrared and Raman assignments were further addressed by ^{13}C and ^{15}N isotope labeling in the imidazolinone ring and the −C═C bridging carbon for neutral, cationic, and anionic HBDI.[2] Together, these studies have established reliable assignments for neutral and anionic HBDI in the high-frequency region 1700−1430 cm^{-1} of the infrared spectra that may be used for mode assignments of chromophore related vibrations in GFP.

Here, we report the picosecond time-resolved mid-infrared absorption changes with optical excitation of the *A* state of GFP that probes the structural response of the protein as well as the chromophore band changes during the fluorescence photocycle. In addition, we have used the pump−dump−probe technique[9,24−26] to determine the $I_2 - I^*$ IR difference spectrum directly.

Materials and Methods

Protein Expression and Purification. GFP−UV (including surface-exposed mutations F99S, M153T, and V163A)[27] was expressed and purified as previously described.[7] Transient optical[9] and steady-state infrared[14] studies show the same spectroscopic properties for wild type GFP and GFP−UV. The E222D mutation was created using the Quickchange (Stratagene) protocol using the primers CATGGTCCTTCTTGACTTTG-TAACTGCTGCTGGG and CCCAGCAGCAGTTACAAAGT-CAAGAAGGACCATG.

Data Collection and Sample Condition. Picosecond time-resolved pump−probe infrared measurements were carried out at the PIRATE facility at the Rutherford-Appleton Laboratory.[28] The 400 nm second harmonic of a 1 kHz titanium:sapphire laser was used to excite samples placed between CaF_2 windows in a 10−20 μm path length Harrick infrared cell. The pump beam was 150 μm in diameter and was attenuated to 2 μJ/pulse. The 100 nJ IR probe pulses with a 150 cm^{-1} fwhm were generated by difference frequency mixing of the signal and idler of an optical parametric amplifier in a type I $AgGaS_2$ crystal and separated into probe and reference beams. Two CVI DKSP240 1/4 m spectrometers disperse the IR beams, using an 150 lines/mm, 4000 nm blaze gold grating. The dispersed IR beams were imaged onto two separate 64 element mercury cadmium telluride MCT-13-64el photoconductive detectors (Infrared Associates Inc.) used together with MCT-64000 preamplifiers (Infrared Systems Development Corp.). The spectral dispersion separating subsequent channel was 11.6 nm, and data were collected in separate overlapping ~200 cm^{-1} windows. The polarization of the probe was set at a magic angle (55°) to the pump. Spectral calibration was carried out by matching the probe arm spectrum to an atmospheric water FTIR spectrum in the same spectral region. Vibrational cooling and coherence effects occurred within the first 2 ps after excitation and are not further addressed in this paper.

To avoid photodegradation and limit phototransformation of GFP and the E222D mutant, the sample was raster scanned in the *x* and *y* directions in an ~1 cm^2 area. Typically, 7 μL of GFP and E222D samples at a 4−8 mM concentration in 5 mM Tris/HCl pH(D) 7.8 in H_2O (D_2O) was used to collect four time delays, and the total number of 400 nm shots was limited to 2×10^5 in five cycles of 20 s acquisitions for each delay at a repetition rate of 500 Hz. Photoconversion[7] as determined by UV−vis spectroscopy was less than 10% after data acquisition. A kinetic dataset in the carbonyl region centered at 1666 cm^{-1} was assembled using data from several samples and scale factors taken from the amplitude at 50 ps (500 ps) at 1721 cm^{-1} (1711 cm^{-1}) in H_2O (D_2O) included in each set. A full kinetic dataset between 1250 and 1800 cm^{-1}, using 25 delays up to 2 ns, was recorded for a 12 mL, 1.7 mM GFP sample in 5 mM Tris/HCl pD 7.8 in D_2O, which flowed in a closed circulating system. The sample was rastered as for the static samples, the path length was 24 μm ($OD_{400} = 0.12$), and the absorption of the amide I band (1650 cm^{-1}) was ~ 0.5. UV−vis spectroscopy and repeated transient IR data acquisition confirmed that no appreciable photodegradation and phototransformation had oc-

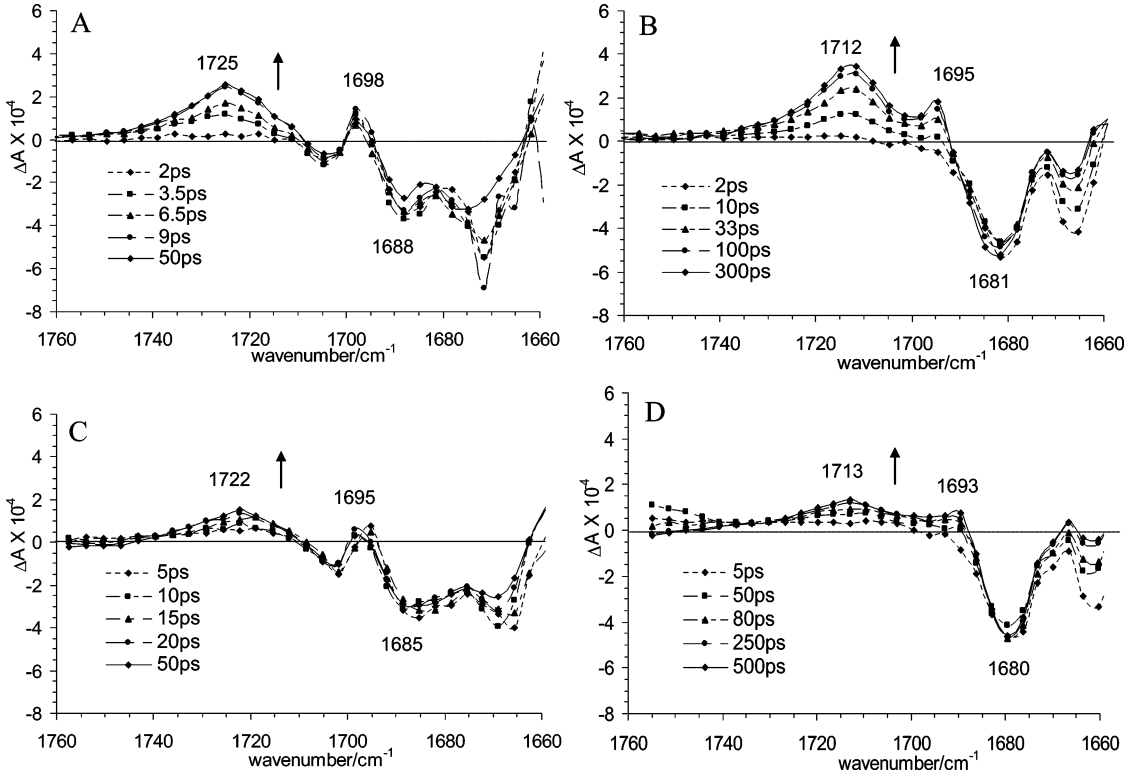

Figure 1. Kinetic difference spectra in the carbonyl region 1760−1660 cm^{-1} for wild type and E222D in H_2O and D_2O. (A) Transient absorption of GFP in H_2O, representing selected traces with delays of 2, 3.5, 6.5, 9, and 50 ps. (B) Data for GFP in D_2O, with selected traces with delays of 2, 10, 33, 100, and 300 ps. (C) E222D mutant in H_2O, with selected traces at 5, 10, 15, 20, and 50 ps. (D) E222D mutant in D_2O, showing traces at 5, 50, 80, 250, and 500 ps. Arrows indicate the direction of change with time.

TABLE 1: Kinetics and Band Positions for Transients Assigned to E222, D222, and Q69 of GFP and the E222D Mutant in H_2O and D_2O[a]

	GFP E222	GFP Q69	E222D D222	E222D Q69
H_2O	$\sigma = 1725\ cm^{-1}$	$\sigma = 1698\ cm^{-1}$	$\sigma = 1722\ cm^{-1}$	$\sigma = 1695\ cm^{-1}$
	$\tau = 5.0 \pm 0.4$ ps	$\tau < 1$ ps	$\tau = 13 \pm 6$ ps	$\tau < 1$ ps
D_2O	$\sigma = 1712\ cm^{-1}$	$\sigma = 1695\ cm^{-1}$	$\sigma = 1713\ cm^{-1}$	$\sigma = 1693\ cm^{-1}$
	$\tau = 22.2 \pm 1.8$ ps[b]	$\tau = 32.7 \pm 5.3$ ps[b]	$\tau = 125.5 \pm 24.1$ ps	$\tau = 35.4 \pm 8.7$ ps

[a] Rise time constants were determined using the approximation of monoexponential fitting allowing comparison of the overall rates. Data for GFP (Figure 1A,B) included 17 time delays between 0 and 50 ps in H_2O and 21 time delays between 0 and 500 ps in D_2O. Nine time delays in H_2O and 18 in D_2O were used for the E222D mutant (Figure 1C,D). [b] Global analysis of data between 1250 and 1800 cm^{-1} revealed two time constants for the excited-state deuteron transfer, 10 and 75 ps.

curred during data collection. These data were recorded in four overlapping separate spectral windows centered at 1666, 1515, 1408, and 1328 cm^{-1} and were interleaved without scaling. The temperature was maintained at 21 °C.

Pump−dump−probe spectroscopy[9,24−26] was realized by including 532 nm pulses resonant with the *I** state from the second harmonic of an ACE AOT_YVO_2QSP/MOPA Nd:YVO_4 laser operated at 1000 Hz, delivering 0.5 ns pulses with 7 μJ/pulse, which were electronically timed to arrive ∼500 ps after the pump. The 532 nm dump pulses were chopped to 500 Hz, and the delay was scanned in 100 ps steps to maximize the overlap with a transient population of the *I** state by maximizing the dump-on minus dump-off pump−probe difference spectrum with the probe delay line set at 1000 ps. The polarization of the dump-pulse was at 20° relative to the pump pulse polarization, and dumping was found to be saturating at the power used. The polarization angle dependency was investigated with orthogonal, parallel, and magic angle orientations of both dump and pump pulses relative to the probe. Data were collected in six separate spectral windows, centered at 1650.5, 1613.0, 1516.4, 1486.6, 1401.0, and 1325.3 cm^{-1}. Data were scaled to the most intense window to provide the amplitudes relevant to the most efficient dump experiment. Sample conditions were 1.7 mM GFP−UV in 5 mM Tris/HCl pD 7.8 in D_2O with a path length of 24 μm, and the sample was flowing in a closed circulating system, as described previously.

Results

Transient Infrared Absorption in the Carbonyl Region 1760−1660 cm^{-1}. Optical excitation of the *A* state of GFP at 400 nm led to transient infrared difference absorption signals in the 1760−1660 cm^{-1} carbonyl region (Figure 1). In H_2O, 50 ps after excitation two major positive bands were detected at 1725 and 1698 cm^{-1}, which were previously assigned to transient protonation of Glu 222 and structural perturbation of Gln 69[14] (Figure 1A). In H_2O, the positive transient at 1698 cm^{-1} was essentially instantaneous within the time resolution of the instrument (Figure 1A and Table 1). The rise kinetics of the positive bands were strongly isotope dependent (Table 1), and their frequencies were downshifted from 1725 to 1712 cm^{-1} and from 1698 to 1695 cm^{-1}, respectively. Using the approximation of monoexponential fitting of the single wavelength kinetic traces, the kinetic isotope effects could be assessed (Table

1). An instantaneous bleach at 1688 cm^{-1} was detected in H_2O and shifted to 1681 cm^{-1} in D_2O.

To definitively assign the 1725/1712 (H_2O/D_2O) cm^{-1} transients and identify the excited-state proton acceptor, glutamate 222 was replaced with aspartate, resulting in the E222D mutant. The UV−vis absorption spectrum of the E222D mutant showed a single maximum at 397 nm, in contrast to the absorption spectrum of GFP, which is characterized by an additional minor absorption at 475 nm belonging to the anionic *B* state.[4] The fluorescence emission of the mutant with 400 nm excitation has a maximum at 508 nm, 2 nm red-shifted with respect to GFP. The fluorescence quantum yield was 0.76, slightly reduced relative to that of GFP taken to be 0.79.[3] The wavelength and quantum yield of the fluorescence emission of the E222D mutant showed that the excited-state proton-transfer reaction is operative as in the wild type. Transient infrared absorption of the E222D mutant revealed detectable changes in the kinetics as well as the position of the bands in the carbonyl region (Table 1). Protonation of Asp 222 gave rise to transients at 1722 cm^{-1} in H_2O and 1713 cm^{-1} in D_2O (Figure 1), and the bands attributed to structural perturbation of Gln 69 were found at 1695 and 1693 cm^{-1}. In addition, both in H_2O and in D_2O, the amplitudes of the 1722 and 1713 cm^{-1} transients of protonated Asp 222 were significantly reduced as compared to Glu 222 in the wild type, when normalized to the 1695(+)/1685(−) cm^{-1} peak/trough.

Photocycle Intermediate Vibrations. To probe the transient absorption changes relevant for the photocycle intermediates *A*, *A**, *I**, and I_2[4,9] in the 1800−1250 cm^{-1} region, time-resolved data were collected up to 2 ns after excitation. Singular value decomposition (SVD) was carried out, revealing three significant spectral components (Figure 2). The SVD time traces could be fitted with three time constants: 10 ps, 75 ps, and 1.7 ns (Figure 2A). The 10 and 75 ps components correspond to the decay of the A_1* and A_2* states, in agreement with transient optical studies,[4,9] whereas the 1.7 ns component corresponds to the decay of the *I** radiative state. The latter time constant is under determined considering data extending to 2.0 ns and may additionally have been affected by a change in optical alignment at long delays. Global fitting of the data using these time constants produced the associated amplitude spectra. From transient optical measurements, the lifetime of the *I** state, 3.0 ns, is well-established, as is the 5.0 ns lifetime of the I_2 ground-state photocycle intermediate that is created with decay of the *I** state in D_2O.[9] Global fitting was also possible with these constants and produced essentially the same amplitude spectra but with larger amplitude for the fourth component. Figure 3 shows the global fits of traces at selected frequencies taking into account a parallel decay of the 10 and 75 ps components. The amplitude spectra for the global fit are presented in Figure 4, which are the difference spectra of the A_1*, A_2*, *I**, and I_2 intermediates relative to the ground-state *A* (Figure 4A−D, respectively). The A_1* − *A* and A_2* − *A* difference spectra are relatively similar as expected but differ significantly in selected regions. The *I** − A_1*, *I** − A_2*, and I_2 − *I** difference spectra are constructed by subtraction and show the absorption changes relevant to the photocycle transitions (Figure 5A−C).

Pump−Dump−Probe Spectroscopy of the *I → I_2 Photocycle Transition.** It has previously been shown from transient optical absorption spectroscopy studies that using a third pulse resonant with *I** efficiently depopulates this radiative singlet state, accelerating the formation of the corresponding ground-state intermediate I_2.[9] The pump−dump−probe experiment[9,24−26] may be used to directly determine the difference spectra

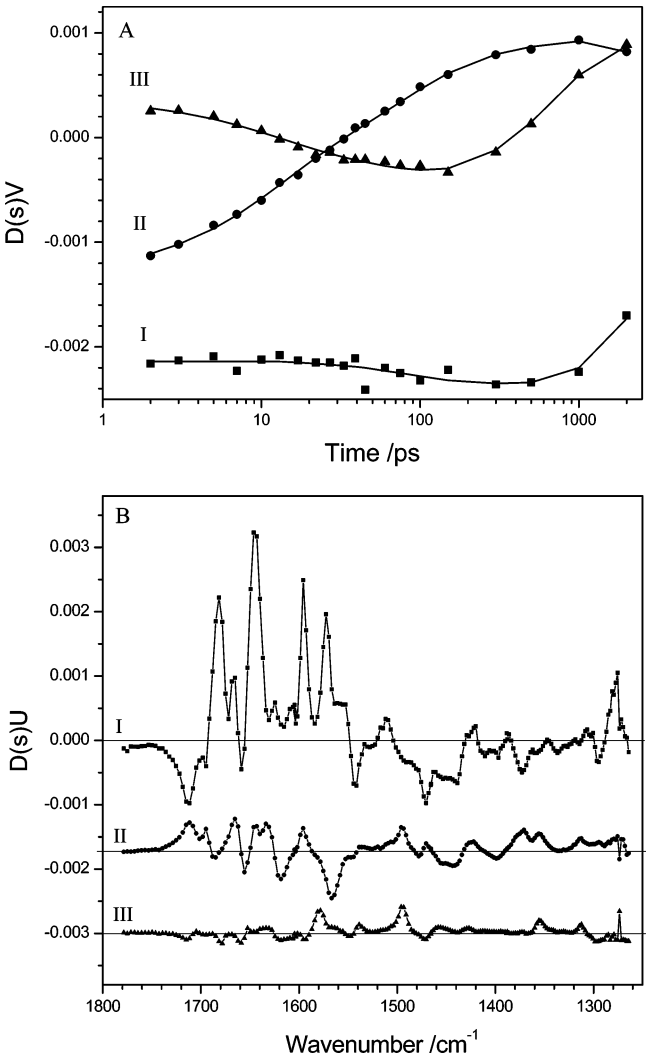

Figure 2. Singular value decomposition (SVD) analysis of the photocycle transient absorption changes of GFP in D_2O. SVD analysis of transient absorption data up to 2 ns between 1800 and 1250 cm^{-1} was carried out according to $\Delta A = UD(s)V^T$. (A) $D(s)V_i(t)$ time traces of the three relevant spectral components I−III with singular values 0.009765, 0.002823, and 0.001369 (■, ●, ▲) were fitted with a sum of three exponentials resulting in $\tau 1 = 10$ ps, $\tau 2 = 75$ ps, and $\tau 3 = 1.7$ ns. (B) Scaled $D(s)U$ SVD basis spectra I−III (■, ●, ▲). 0.0017 ΔOD and 0.003 ΔOD have been subtracted from components II and III, as indicated with baselines.

corresponding to electronic relaxation in addition to accelerating the photocycle transition of GFP. We applied this technique together with the infrared pump−probe experiments to determine the I_2 − *I** difference spectrum directly. During the photocycle, a relatively small population of the I_2 state transiently accumulates in D_2O due to the KIE of the ground-state recovery, whereas in H_2O, this population is negligible.[9] By including a third 532 nm pulse resonant with the *I** optical transition, efficient population of the I_2 intermediate was observed. The I_1 intermediate, which decays in 7 ps,[9] may not be observed in these experiments. Contributions of the *A* state could not be observed on the product side of the pump−dump−probe spectrum consistent with the insignificant decay of the I_2 state with probing within 10% of its lifetime. Figure 6 shows the dump-on minus dump-off difference spectrum between 1800 and 1250 cm^{-1}, which corresponds to the I_2 − *I** difference spectrum. Judged from the amplitude of the most dominant I_2 state band at 1493 cm^{-1} (Figure 6) in comparison with its

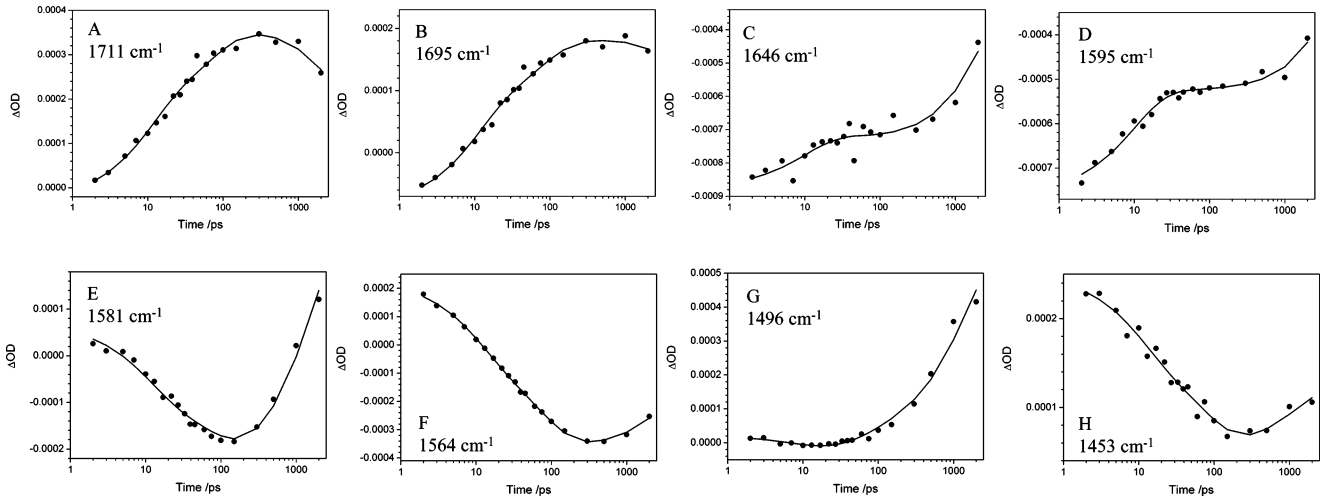

Figure 3. Global fitting of transient absorption traces of GFP in D_2O. Eight out of 202 traces globally fitted with the photocycle model using decay constants of $\tau 1 = 10$ ps, $\tau 2 = 75$ ps, $\tau 3 = 3.0$ ns, and $\tau 4 = 5.0$ ns for the A_1*, A_2*, I*, and I_2 states, respectively, at 1711 cm^{-1} (A), 1695 cm^{-1} (B), 1646 cm^{-1} (C), 1595 cm^{-1} (D), 1581 cm^{-1} (E), 1564 cm^{-1} (F), 1496 cm^{-1} (G), and 1453 cm^{-1} (H).

photocycle counterpart (Figure 5C), the optical dumping was efficient.

Discussion

Transients in the Carbonyl Region 1760−1660 cm^{-1}. Optical excitation of the *A* state produces the *A** state that undergoes rapid excited-state proton transfer, causing the chromophore to become ionized. In the wild type, transient absorption is observed at 1725/1712 cm^{-1} (H_2O/D_2O) that belongs to a carboxylic acid group acting as a transient proton acceptor[14] (Figure 1 and Table 1). This observation suggests that Glu 222 acts as the terminal proton acceptor, in agreement with some previous proposals.[17,18] A recent study showed a similar measurement, although with the transient at 1706 cm^{-1} and no corresponding data in H_2O, also suggesting Glu 222.[19] In view of a recent proposal for a proton-transfer pathway including Glu 222, Asp 82, and Glu 5,[21] the transient in the carboxylic acid region may also be attributed to Asp 82, Glu 5, or a superposition of bands belonging to multiple carboxylic acid groups. To definitively assign this band, Glu 222 was replaced by Asp. The E222D mutant protein showed efficient excited-state proton transfer as the wild type, but transient absorption in the high-frequency region was affected with respect to the absorption frequency, rise kinetics, and band intensities both in H_2O and in D_2O (Figure 1 and Table 1). This evidence strongly favors assignments to Asp 222 in the mutant as the excited-state proton acceptor, and by inference, Glu 222 in the wild type. By contrast, other replacements at position 222 such as Gln[19] will not create *A* state GFP variants, and the transient absorption therefore cannot contain contributions from an excited-state proton-transfer reaction.

The H/D kinetic isotope effect (KIE) for the proton transfer reaction was approximately 4.4 (Table 1), similar to the value of 6 determined from transient optical spectroscopy.[4,9] The KIE of this transfer reaction may be explained using the traditional semiclassical transition-state theory taking into account the zero-point energy for the hydrogen and deuterium stretch vibrations along the reaction coordinate together with classical barrier crossing.[29] The KIE for the 1698/1695 cm^{-1} (H_2O/D_2O) band assigned to Gln 69[14] is very high (>32). In H_2O, the transient is observed within 1 ps after excitation and is therefore an *A** mode (Figure 1 and Table 1). With H/D exchange, however, this mode kinetically tracks with the 1711 cm^{-1} Glu 222 band, and so converts it to an *I** mode. The H/D KIE therefore exceeds 32, which could normally be taken as an indication of tunneling behavior.[29] However, since the transient is assigned to structural perturbation of Gln 69 on the basis of mutagenesis and X-ray crystallography,[14] this structural motion strongly depends on the active site vibrations, which could be the H/D stretch vibrations along the reaction coordinate.

Photocycle Intermediate Vibrations. Through SVD analysis and global fitting, the difference spectra of the photocycle intermediates relative to the ground state were determined, including the late I_2 ground-state intermediate, which was recently discovered.[9] The 10 and 75 ps components belong to parallel $A^* \rightarrow I^*$ transitions, which are accompanied by excited-state proton transfer. In very close agreement with the transient infrared absorption data, optical pump−probe spectroscopy has identified 12 ps (42%) and 69 ps (58%) time constants for this step in D_2O (and 2.2 ps (49%) and 11.1 ps (51%) in H_2O).[9] We found that single wavelength traces may not readily support fitting with two exponentials without such prior knowledge, and consequently, we present our E222D mutant data with the approximation of monoexponential fitting, allowing comparison of the overall rate changes (Table 1). In contrast, the SVD analysis of the 202 time traces for the wild type in D_2O clearly supported the two constants for the *A** decay (Figure 2). Global analysis was performed imposing a reaction model for the parallel $A^* \rightarrow I^*$ transformations with 10 and 75 ps time constants, an *I** lifetime of 3.0 ns,[4,9] forming I_2 that has a lifetime of 5.0 ns.[9] The accuracy of the global fit is evident from eight selected time traces at frequencies corresponding to ground-state and intermediate vibrations (Figure 3).

Assignment of the major bands may be proposed based on the published assignments of the infrared absorption bands of the neutral and anionic form of the model compound 4-hydroxybenzylidene-1,2-dimethylimidazolinone (HBDI) in dimethyl sulfoxide (DMSO)[2] and in KBr,[1,30] in combination with isotope substitutions[2] and calculation of infrared transition frequencies and intensities.[1,2,30] In addition, nonresonance Raman and resonance Raman spectroscopy data and calculations with corresponding assignments for the Raman frequencies are available.[1,2,30] The $A_1^* - A$ and $A_2^* - A$ difference spectra presented in Figure 4A,B show negative bands that belong to the ground state, for which mode assignments are proposed (Table 2). These bands are similarly observed in the $I^* - A$

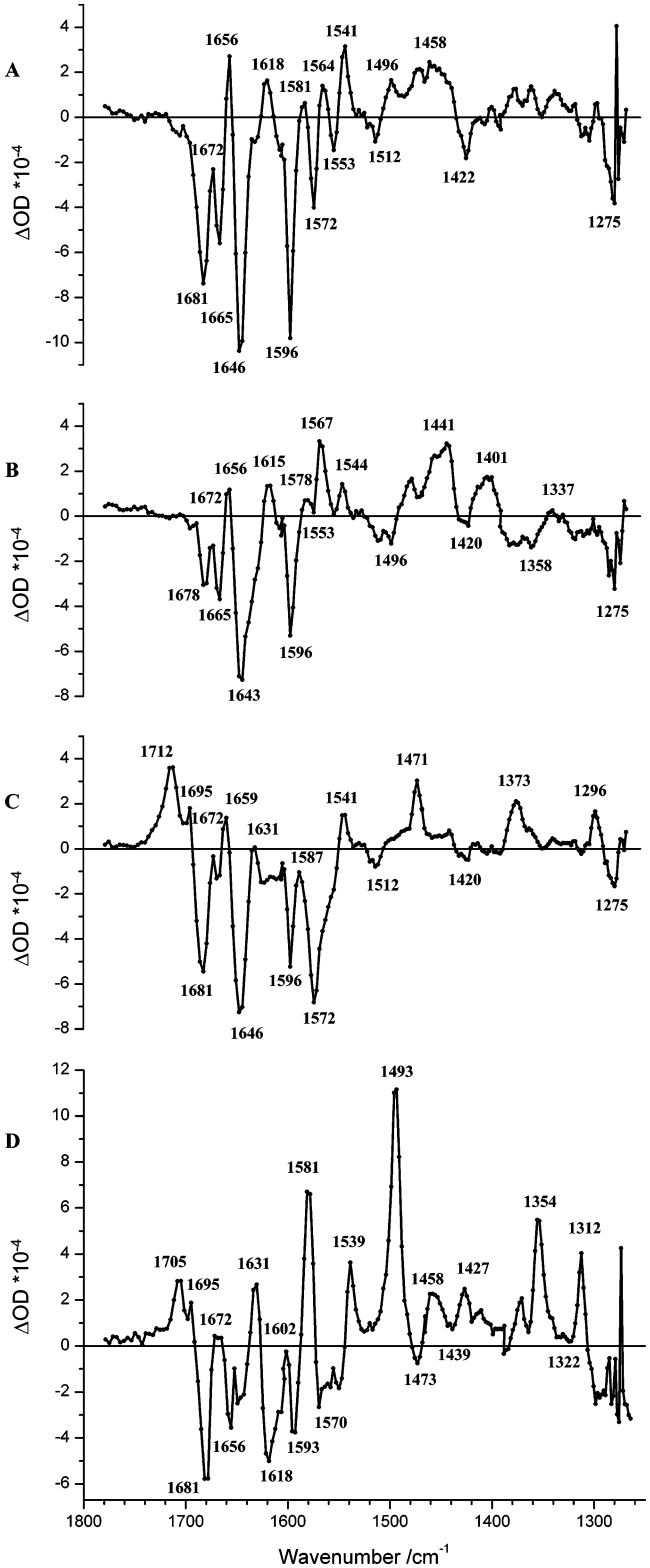

Figure 4. Time-independent difference spectra for the global fit of transient absorption of GFP between 1800 and 1250 cm^{-1} in D_2O. Difference spectra relative to the ground state are presented for the parallel $\tau1 = 10$ ps and $\tau2 = 75$ ps components and the consecutive I^* and I_2 states with $\tau3 = 3.0$ ns and $\tau4 = 5.0$ ns lifetimes, resulting in the $A_1^* - A$ (A), $A_2^* - A$ (B), $I^* - A$ (C), and $I_2 - A$ (D) difference spectra.

and $I_2 - A$ difference spectra (Figure 4C,D). Strikingly, the $I_2 - A$ difference spectrum (with the exception of the 1705 and 1695 cm^{-1} bands) strongly resembles the $GFP_R - GFP_A$ static FTIR difference spectrum determined with phototransformation

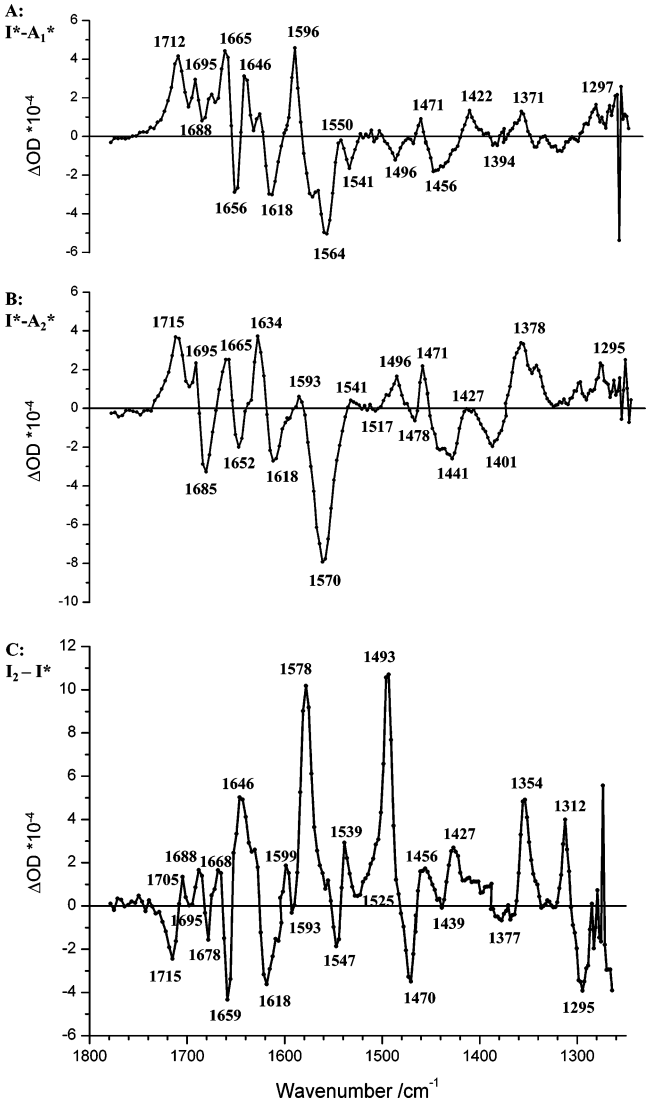

Figure 5. Constructed time-independent difference spectra for the photocycle transitions of GFP in D_2O. Spectra are constructed by subtraction to give the $I^* - A_1$ (A), $I^* - A_2^*$ (B), and $I_2 - I^*$ (C) difference spectra.

of wild type GFP, which correspond to the neutral and anionic ground-state species.[7,14] These similarities extend to small features as well, further supporting the accuracy of the amplitude determination of the intermediate spectra by global fitting as shown in Figure 3. Assignments of I_2 vibrations may be proposed as for the ground-state bands, based on the observed band shift and the published model compound assignments. It is noted that for all high-frequency bands addressed in these assignment strategies, there is a downshift observed for all modes concomitant with deprotonation of the phenolic chromophore,[1,2,30] consistent with the expected bond order reduction. The general downshift character of the experimental $I_2 - A$ difference spectrum (Figure 4D) additionally substantiates this observation. Mode assignments are proposed for the A_1^*, A_2^*, and I^* excited-state intermediates based on the generally expected downshift relative to their respective ground states through the reduction of bond orders. It is noted that the $I^* - A^*$ difference spectra (Figure 5A,B) also exhibit a downshift character in the high-frequency region, similar to the downshift pattern observed in the $I_2 - A$ difference spectrum (Figure 4D).

The C═O stretch of protonated Glu 222 as well as the C═O band of Gln 69 are shown to be I^* bands, and their absorption bands are kinetically correlated with chromophore bands.

TABLE 2: Assignments of A_1/A_2 and I_2 Ground-State Modes and Tentative Assignments to Photocycle Intermediates A_1*, A_2*, and I*[a]

	mode	A_1	A_1*	A_2	A_2*	I*	I_2
E222	COOH					1712	1705
Q69	C═O		1688		1685	1695	1695
1	C═O	1681	1672	1678	1672	1672	1672
A	C═C (chromophore) or C═O (protein)	1665	1656	1665	1656/1652	1646	1668
2	C═C	1646	1618	1643	1615	1631/1634	1631/1646
3	phenol 1	1596	1581	1596	1578	1587	1578/1581
4	phenol 2	1572	1564	1572	1567/1570	1547	
E222	COO^-(asym)		1564		1570		
5	C═N and C═C	1553	1541	1553	1544	1525/1541	1539
6	phenol 3	1512	1496	1496	1476	1471	1493
E222	COO^- (sym)		1456		1441		
7	^{13}C5-sensitive					1373	1354
8	Phenol	1275		1275		1297/1295	1312

[a] Modes 1−6 are numbered according to refs 1 and 2. A novel unidentified C═C mode is designated *A*, and its assignment is tentatively made to a C═C chromophore or a C═O protein vibration. Modes 1−8 assignments are proposed for the A_1/A_2 and I_2 ground states based on refs 1 and 2, and their dominant character is listed. E222 and Q69 assignments for the *I** state are according to ref 14. Tentative assignments for the excited-state intermediates A_1*, A_2*, and *I** chromophore vibrations are proposed. Peaks from bandshift features in different spectra referring to the same mode are given together separated with a slash. The absence of corresponding vibrations in the spectra is indicated with a blank cell.

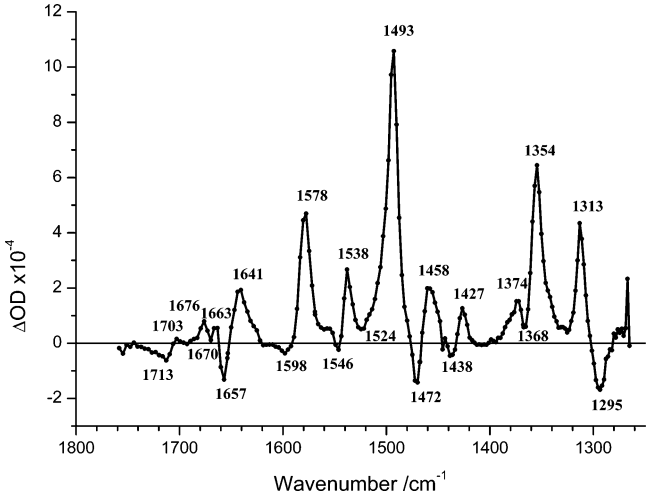

Figure 6. Pump−dump−probe spectrum of the *I** intermediate. Dump-on minus dump-off pump−probe spectrum with the optical delay line set at 1 ns and the 500 ps 532 nm pulse timed to arrive ∼500 ps after excitation produces the $I_2 - I$* spectrum directly.

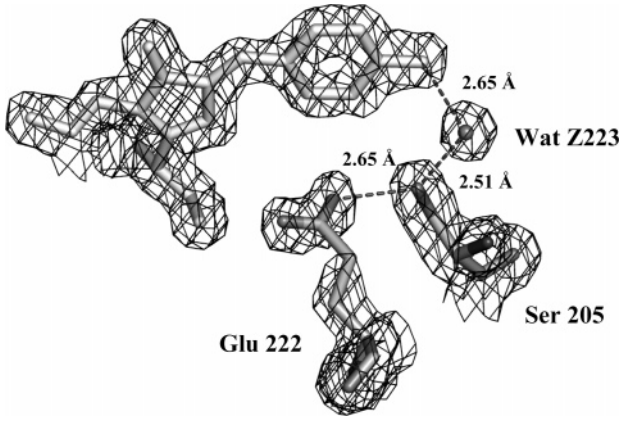

Figure 7. Structural disorder of Glu 222 in the *A* state. $2F_o - F_c$ electron density difference map of an *A* state X-ray structure determined at 1.85 Å resolution, with contouring at 1.6σ showing structural disorder of the Glu 222 side chain. Drawn from 1W7S.[14]

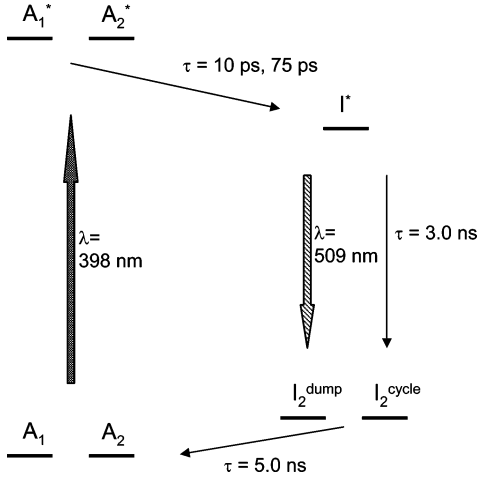

Figure 8. Energy level diagram for the photocycle transitions and kinetics of GFP in D_2O. The structural heterogeneity of the *A* and *A** states is indicated, and a distinction is made between the I_2 ground-state intermediate accumulated in the photocycle (I_2^{cycle}) and the corresponding state formed by optical dumping (I_2^{dump}). Optical transitions are shown with large arrows, whereas thermal and radiative decay is indicated with thin arrows.

However, with the formation of the I_2 late intermediate, the intensity of the protonated Glu 222 band is significantly decreased, and its maximum is downshifted by 7 cm^{-1}, signaling either increased hydrogen bonding and a reduced protonation level[31] or proton transfer to a new species altogether (Figure 4D, 5C and Table 2). The increased hydrogen bonding is in line with the observed solvent reorientations and formation of a hydrogen bonding network following chromophore ionization[14] and argues against a late intermediate *I* state structure with decreased H-bonding, which was predicted on the basis of molecular dynamics simulations.[32] Assuming a decreased protonation level of Glu 222 in the I_2 state relative to the *I** state, it is concluded that partial proton transfer to an intermediate acceptor occurs. The identity of the acceptor may be either Ser 205 or water Z223, which is likely to take part in the forward transfer to Glu 222 (Figures 7 and 8). An alternative explanation may involve proton transfer through a pathway including Glu 222, Asp 82, and Glu 5, although postulated to occur during the lifetime of the *I** state.[21] The observation of an intermediate acceptor may explain the inflated H/D KIE of 12 for the reprotonation reaction[9] rather than tunneling.

With regard to the expected asymmetric COO^- stretching vibration of deprotonated Glu 222, this could be present in the bleach at 1564 and 1570 cm^{-1} bands in the *I** − A_1* and *I** − A_2* spectra, respectively (Figure 5A,B), as suggested previously.[19] However, absorption band changes in this region are assigned to belong to mostly the phenol 2 mode (mode 4, Table

2). In addition, the $I^* - A_1^*$ difference spectrum (Figure 5A) has a bandshift character in this region and also shows significantly less intensity than the corresponding feature in the $I^* - A_2^*$ spectrum (Figure 5B). Furthermore, the $I_2 - I^*$ difference spectrum, which shows a bleach at 1715 cm^{-1}, does not show corresponding positive absorption at this frequency, although this may be masked by the strong phenol 1 mode (mode 3, Table 1). It is likely that the asymmetric COO^- stretch bands and the phenol 2 and phenol 1 bands superimpose in the $A^* \rightarrow I^*$ and $I^* \rightarrow I_2$ transitions, respectively. The $I_2 - A$ difference spectrum (Figure 4D) is dominated by strong positive phenolate modes in this region, and no convincing bleach signal may be assigned to the COO^- stretching in this spectrum or in the phototransformation induced ground-state difference spectra published previously.[7,14] A more isolated mode is observed at 1456 and 1441 cm^{-1} in the $A_1^* - A$ and $A_2^* - A$ difference spectra, respectively, which is tentatively assigned to the low-frequency symmetric stretch vibrations of the Glu 222 COO^- group (Figure 5A,B). Supporting this proposal, a positive band at 1456 cm^{-1} is observed in the $I_2 - I^*$ difference spectrum, which could correlate with the recovery of the ionized COO^- group. The intensities of these bands are comparable with their corresponding high-frequency C═O signals for protonated Glu 222, in agreement with their comparable extinction coefficients.[31] Alternatively, this band could correspond to the 1434 and 1438 cm^{-1} Raman bands for neutral and anionic HBDI in D_2O, which were assigned to the C−C−H in-plane deformation of the phenol ring.[2]

The C═O band of the chromophore (mode 1, Table 2) is present as a strong bleach already in the $A^* - A$ difference spectra (Figure 4A,B), and assignments for the corresponding downshifted modes in the photocycle intermediates are proposed based on the expected bond order reductions and model compound behavior[2] (Table 2). Assignment of this mode was already proposed for the *A* state previously.[19] Other strong modes in this part of the spectra are found to belong to the chromophore C═C (mode 2) and phenol 1 (mode 3). These modes have been found to be more delocalized but are referred to by their dominant contribution[1,2] (Table 2). Raman spectroscopy has identified mode 2 at 1645 and 1630 cm^{-1} for the neutral and anionic states, respectively,[33] in agreement with the band positions in the *A* and I_2 state of the transient infrared absorption.

An additional high-frequency ground-state mode was observed that is not reported in model compound studies and is also not predicted by electronic structure calculation methods.[1,2,30] All intermediate spectra show bands for this mode, which is labeled mode A (Table 2 and Figures 4 and 5). This labeling was proposed assuming a bandshift feature for this additional mode, but an alternative interpretation invokes a narrow positive (A^*) band at 1672 cm^{-1}, effectively cutting a broad negative *A* state band to produce two separate minima at 1680 and 1665 cm^{-1}, belonging to mode 1 (Table 2). This interpretation would fit with the observation of a broad negative (*A* state) band observed in static $GFP_R - GFP_A$ FTIR spectra at 1674 cm^{-1}.[7,14] Both interpretations of the difference spectra involve infrared active vibrations, which are unique to the photocycle of GFP and are also not observed in the phototransformation FTIR difference spectra at low or high temperatures.[14] This mode is present in all spectra and might therefore be a new chromophore vibration, possibly a C═C mode, belonging to an alternative conformation. However, this is not visibly reflected in other chromophore modes. The alternative possibility of a protein contribution, also in the $A \rightarrow A^*$ transition, would suggest a Gln or Asn C═O vibration, or alternatively Arg.[31] Definitive assignment is therefore not possible, but its appearance in the early spectra tentatively suggests it to be a chromophore mode.

Mode 5 is a chromophore mode that has been shown from isotope studies to be delocalized and contains contributions of both chromophore C═N and C═C vibrations,[2] which is also confirmed by its absence in difference spectra for model compounds of protonated and anionic photoactive yellow protein.[7] This mode is identified in the *A* state as well as the I_2 state, and band assignments for the intermediates are proposed (Table 2). A phenol mode (mode 7, Table 2) is assigned in the *A*, I^*, and I_2 states that is known to shift up with ionization of phenolic compounds, from 1244 to 1270 cm^{-1} in the case of poly(L-tyrosine).[7,34,35] No corresponding mode could be proposed for the A^* states, but strong upshifted I^* and I_2 modes were observed (Figures 4 and 5 and Table 2).

Structural Heterogeneity and Relaxation in the Photocycle. A correlation has been shown between the frequency of mode 2 for anionic states and the electronic absorption energy.[33] It was proposed that through interaction with the protein environment, the resonance frequency of both the C═C mode (mode 2) as well as the electronic transition reflect ground-state changes. By this criterion, the observed band position at 1631 cm^{-1} for the C═C mode in the I_2 state (mode 2, Table 1) shows the chromophore to be in an intermediate environment, comparable to anionic HBDI in DMSO,[2] 9 cm^{-1} downshifted from anionic HBDI in KBr.[30] The electronic absorption of I_2 at 497 nm and the 1631 cm^{-1} frequency for mode 2 fits reasonably with the published correlation.[33]

Structural relaxation of the chromophore and protein environment upon chromophore ionization was observed after phototransformation at cryogenic temperatures.[14] The early photoproduct generated at 100 K showed a red-shifted absorption maximum (497 nm) relative to the fully relaxed photoproduct created at 300 K (477 nm).[14] The structural relaxation with thermal annealing was accompanied by a significant downshift of a phenolate specific mode from 1362 to 1341 cm^{-1}.[14] Here, a correlation between a decrease of the vibrational transition energy of mode 7 and an increase of the electronic transition energy was observed, coinciding with structural relaxation. This mode is also found in the I_2 photocycle intermediate at a frequency, 1354 cm^{-1}, intermediate between the extreme values observed in the phototransformation pathway, and a corresponding I^* vibration is proposed (mode 7, Table 2). The frequency of this mode in the I_2 intermediate shows that the chromophore is not fully structurally relaxed, which is also in line with the relatively low energy optical transition (497 nm). No specific character has been assigned to mode 7 but it is likely to contain phenol ring motions and appears to be sensitive to ^{13}C isotope substitution at C5 but not at the neighboring atoms $^{13}C\alpha$, $^{13}C1$, and $^{15}N4$.[2]

The presence of the 1695 cm^{-1} band assigned to Gln 69 in both the I^*[14] and the I_2 intermediates suggests that the fluorescence photocycle intermediates are similar to the early phototransformation intermediates GFP_L and GFP_M and that both the frequencies of the optical absorption, the Gln 69 band and mode 7, suggest that the I^* and I_2 states are structurally unrelaxed and intermediate between the GFP_L and the GFP_M states.

The pump−dump−probe $I_2 - I^*$ difference spectrum strongly resembles the $I_2 - I^*$ difference spectrum globally fitted from the transient absorption photocycle measurements but appears to be characterized by somewhat weaker I^* bands. The transient

population of the I_2 intermediate at a late time in the photocycle may have been slightly underestimated as judged from the directly determined difference spectrum. Further, the phenol 1 mode at 1578 cm^{-1} in the dumped I_2 state is significantly less intense than its photocycle counterpart (Figure 5C and Figure 6). Comparison of the intensities of the 1578 and 1498 cm^{-1} bands detected in single spectral windows showed this to be a genuine difference between the I_2 state created by optical dumping and the I_2 photocycle intermediate. The ratio between the 1578 and 1498 cm^{-1} band intensities was independent of the polarization angles of both the dump and the pump pulses relative to the probe pulses. With conventional pump−probe spectroscopy using a 2 ns delay, the ratio between the I_2 photocycle intermediate bands was also shown to be independent of the polarization angle between pump and probe pulses, indicating that the transition dipole moments of the phenol 1 and phenol 3 modes are relatively well-aligned. The phenol 1 mode is a strongly infrared active and also Raman active out-of-plane phenol deformation mode with small contributions from the imidazolinone C═N stretching vibrations.[1,2] Its reduced intensity points to a stronger delocalization of the negative charge onto the phenolic ring of the anionic chromophore causing reduced aromaticity in the case of the dump-generated I_2 state. Furthermore, the bandshift feature assigned to the chromophore C═O mode (mode 1) is found at a lower frequency in the dumped I_2 state, additionally suggesting a branching reaction model rather than an acceleration for the optical dumping of the I^* state (Figure 8). From transient optical measurements, it appeared that the 5 ns lifetimes of the dumped and photocycle I_2 states are comparable in D_2O.[9] Reprotonation is likely to be rate limiting for this last step in the photocycle.

The spectra belonging to the 10 and 75 ps time constants (Figure 4A,B) are similar, but some striking differences are obvious. In particular, the $A_2^* - A$ difference spectrum (Figure 4B) is characterized by a significantly reduced shift character for mode 1 corresponding to the chromphore C═O vibration. Differences in the lower frequency region are also notable, with stronger contributions around 1400 cm^{-1} in the A_2^* state (Figure 4A,B). Comparing the $I^* - A_1^*$ (Figure 5A) and the $I^* - A_2^*$ (Figure 5B) difference spectra, a difference in intensity of the 1570 cm^{-1} A_2^* band was assigned to mode 4 with possible contributions from Glu 222 COO^- asymmetric stretch vibrations, relative to the corresponding 1564 cm^{-1} A_1^* band. Interestingly, the bleaches at 1456 and 1441 cm^{-1} tentatively assigned to the Glu 222 COO^- symmetric stretch vibrations are found at different frequencies. We speculate that this difference could reflect structural disorder of the Glu 222 side chain and present X-ray crystallography data that supports disorder in the A state (Figure 7). In the ground state, discontinuous electron density is observed in particular for the CG and CB carbon atoms of the Glu 222 side chain at a 1.6σ contouring level, signaling increased disorder for these atoms. In the refined coordinates, the side chain is not in a rotamer conformation but is characterized by the angles $\chi_1 = 62°$, $\chi_2 = 153°$, and $\chi_3 = -145°$.[14] The X-ray data indicate the presence of other unrelaxed conformations that could contribute to the parallel excited-state deprotonation reactions. We suggest a reaction model that is distinctly different from published theoretical models proposing relaxed (syn) and unrelaxed (anti) conformations of protonated Glu 222 in the I ground state[17,32] and take into account different side chain conformations in the ground state based on the different frequencies of the COO^- vibrations in the first two kinetic components as well as the disorder inferred from the electron density. Additionally, the chromophore modes are indicative of structural heterogeneity of the chromophore and its environment in the A_1^* and the A_2^* states and only partial relaxation in the late intermediate I_2. In this context, it is interesting to note that increased structural disorder of solvent and specific side chains, including Gln 69, relative to the A state was observed in the X-ray structure of the cryogenically trapped GFP_L lumi state, which resembles the I^* photocycle intermediate.[14] This suggests that the I^* state may be structurally disordered as well.

Conclusions

A detailed study of the structural events in the photocycle of GFP is presented. Definitive evidence for the proton transfer pathway to Glu 222 in the $A^* \rightarrow I^*$ transition is provided from the transient infrared absorption spectroscopy of the E222D mutant, but partial proton transfer to unidentified intermediate acceptors later in the photocycle is clearly observed, suggesting local proton trapping to be underlying of the inflated KIE of reprotonation of the chromophore. The electrostatic response to optical excitation causes structural rearrangements of solvent and specific side chains including Gln 69, to which infrared absorption changes were assigned.[14] Here, we show that the structural perturbation of Gln 69 is strongly dependent on the H/D vibrations, and we hypothesize that the motions are vibrationally coupled to the H/D stretch vibrations along the proton-transfer coordinate. SVD and global analysis of the time-resolved transient absorption data support a reaction model including two parallel excited-state deprotonation reactions with time constants of 10 and 75 ps and produce the time-independent difference spectra of the A_1^*, A_2^*, I^*, and I_2 intermediates relative to the ground state. The two $A^* \rightarrow I^*$ transitions are characterized by marked differences in the infrared absorption changes, in particular with regard to the chromophore C═O mode, a phenol 2 mode at 1570 cm^{-1} potentially including Glu 222 COO^- (asym) bleaching, and a mode tentatively assigned to Glu 222 COO^- (syn) at 1456 and 1441 cm^{-1}. These two bands could belong to structurally different A^* states, and indications for similar heterogeneities of the A ground state are also presented on the basis of X-ray data (Figure 8). In D_2O, the transient accumulation at late time points of the I_2 ground-state intermediate is due to the strong KIE for A ground-state reformation. Chromophore modes for the A and I_2 ground states are assigned on the basis of published work, and assignments for the A^* and I^* excited-state intermediates are proposed on the basis of expected bond order changes. A pump−dump−probe experiment directly generating the $I_2 - I^*$ difference spectrum is significantly different from the photocycle spectrum, in particular pointing to reduced aromaticity for the dumped I_2 state relative to the photocycle intermediate. Optical as well as vibrational spectral markers at 1695, 1539, and 1354 cm^{-1} indicate that GFP is unrelaxed even in the long-lived, late photocycle ground-state intermediate I_2, which together with the observation of structural heterogeneity in the reaction cycle provides a picture of the role of the protein environment in the fluorescence of GFP.

Acknowledgment. J.J.v.T. is a Royal Society University Research Fellow. This work was supported through access to the PIRATE facility, Central Laser Facility, Rutherford Appleton Laboratory, Chilton, Didcot, UK (US/22/B/2/04 to J.J.v.T.). We thank Jenny Gibson for technical assistance, Pavel Matousek for help with data collection, Joachim Heberle and Teresa Bednarz for SVD, and Timothy Sage for helpful discussion.

References and Notes

(1) Esposito, A. P.; Schellenberg, P.; Parson, W. W.; Reid, P. J. *J. Mol. Struct.* **2001**, *569*, 25.
(2) He, X. B.; Bell, A. F.; Tonge, P. J. *J. Phys. Chem. B* **2002**, *106*, 6056.
(3) Tsien, R. Y. *Annu. Rev. Biochem.* **1998**, *67*, 509.
(4) Chattoraj, M.; King, B. A.; Bublitz, G. U.; Boxer, S. G. *Proc. Natl. Acad. Sci. U.S.A.* **1996**, *93*, 8362.
(5) Yang, F.; Moss, L. G.; Phillips, G. N., Jr. *Nat. Biotechnol*. **1996**, *14*, 1246.
(6) Cody, C. W.; Prasher, D. C.; Westler, W. M.; Prendergast, F. G.; Ward, W. W. *Biochemistry* **1993**, *32*, 1212.
(7) van Thor, J. J.; Pierik, A. J.; Nugteren-Roodzant, I.; Xie, A.; Hellingwerf, K. J. *Biochemistry* **1998**, *37*, 16915.
(8) Heim, R.; Prasher, D. C.; Tsien, R. Y. *Proc. Natl. Acad. Sci. U.S.A.* **1994**, *91*, 12501.
(9) Kennis, J. T.; Larsen, D. S.; van Stokkum, I. H.; Vengris, M.; van Thor, J. J.; van Grondelle, R. *Proc. Natl. Acad. Sci. U.S.A.* **2004**, *101*, 17988.
(10) Winkler, K.; Lindner, J.; Subramaniam, V.; Jovin, T. M.; Vohringer, P. *Phys. Chem. Chem. Phys.* **2002**, *4*, 1072.
(11) Lossau, H.; Kummer, A.; Heinecke, R.; Pöllinger-Dammer, F.; Kompa, C.; Bieser, G.; Jonsson, T.; Silva, C. M.; Yang, M. M.; Youvan, D. C.; Michel-Beyerle, M. E. *Chem. Phys.* **1996**, *213*, 1.
(12) Förster, T. *Z. Elektrochem.* **1949**, *53*, 42.
(13) Creemers, T. M.; Lock, A. J.; Subramaniam, V. V.; Jovin, T. M.; Volker, S. *Nat. Struct. Biol.* **1999**, *6*, 706.
(14) van Thor, J. J.; Georgiev, G.; Towrie, M.; Sage, T. *J. Biol. Chem.* **2005**, in press.
(15) Seebacher, C.; Deeg, F. W.; Brauchle, C.; Wiehler, J.; Steipe, B. *J. Phys. Chem. B* **1999**, *103*, 7728.
(16) Youvan, D. C.; Michel-Beyerle, M. E. *Nat. Biotechnol.* **1996**, *14*, 1219.
(17) Brejc, K.; Sixma, T. K.; Kitts, P. A.; Kain, S. R.; Tsien, R. Y.; Ormo, M.; Remington, S. J. *Proc. Natl. Acad. Sci. U.S.A.* **1997**, *94*, 2306.
(18) Palm, G. J.; Zdanov, A.; Gaitanaris, G. A.; Stauber, R.; Pavlakis, G. N.; Wlodawer, A. *Nat. Struct. Biol.* **1997**, *4*, 361.
(19) Stoner-Ma, D.; Jaye, A. A.; Matousek, P.; Towrie, M.; Meech, S. R.; Tonge, P. J. *J. Am. Chem. Soc.* **2005**, *127*, 2864.
(20) Leiderman, P.; Ben-Ziv, M.; Genosar, L.; Huppert, D.; Solntsev, K. M.; Tolbert, L. M. *J. Phys. Chem. B* **2005**, *108*, 8043.
(21) Agmon, N. *Biophys. J.* **2005**, *88*, 2452.
(22) van Thor, J. J.; Gensch, T.; Hellingwerf, K. J.; Johnson, L. N. *Nat. Struct. Biol.* **2002**, *9*, 37.
(23) Yoo, H. Y.; Boatz, J. A.; Helms, V.; McCammon, J. A.; Langhoff, P. W. *J. Phys. Chem. B* **2001**, *105*, 2850.
(24) Gai, F.; MacDonald, J. C.; Anfinrud, P. A. *J. Am. Chem. Soc.* **1997**, *119*, 6201.
(25) Changenet-Barret, P.; Choma, C. T.; Gooding, E. F.; DeGrado, W. F.; Hochstrasser, R. M. *J. Phys. Chem. B* **2000**, *104*, 9322.
(26) Logunov, S. L.; Volkov, V. V.; Braun, M.; El-Sayed, M. A. *Proc. Natl. Acad. Sci. U.S.A.* **2001**, *98*, 8475.
(27) Crameri, A.; Whitehorn, E. A.; Tate, E.; Stemmer, W. P. *Nat. Biotechnol.* **1996**, *14*, 315.
(28) Towrie, M.; Grills, D. C.; Dyer, J.; Weinstein, J. A.; Matousek, P.; Barton, R.; Bailey, P. D.; Subramaniam, N.; Kwok, W. M.; Ma, C.; Phillips, D.; Parker, A. W.; George, M. W. *Appl. Spectrosc.* **2003**, *57*, 367.
(29) Kohen, A.; Klinman, J. P. *Chem. Biol.* **1999**, *6*, R191.
(30) Schellenberg, P.; Johnson, E.; Esposito, A. P.; Reid, P. J.; Parson, W. W. *J. Phys. Chem. B* **2001**, *105*, 5316.
(31) Barth, A.; Zscherp, C. *Q. Rev. Biophys.* **2002**, *35*, 369.
(32) Lill, M. A.; Helms, V. *Proc. Natl. Acad. Sci. U.S.A.* **2002**, *99*, 2778.
(33) Bell, A. F.; He, X.; Wachter, R. M.; Tonge, P. J. *Biochemistry* **2000**, *39*, 4423.
(34) Dollinger, G.; Eisenstein, L.; Lin, S. L.; Nakanishi, K.; Termini, J. *Biochemistry* **1986**, *25*, 6524.
(35) Rothschild, K. J.; Roepe, P.; Ahl, P. L.; Earnest, T. N.; Bogomolni, R. A.; Das Gupta, S. K.; Mulliken, C. M.; Herzfeld, J. *Proc. Natl. Acad. Sci. U.S.A.* **1986**, *83*, 347.